46th AIAA Aerospace Sciences Meeting and Exhibit
7 - 10 January 2008, Reno, Nevada

AIAA 2008-22

Experiments on the Effect of Ground Reflections on Supersonic Jet Noise

Dennis K. McLaughlin* and Ching-Wen Kuo†
Penn State University, University Park, PA 16802

Dimitri Papamoschou‡
University of California, Irvine, Irvine, CA, 92697-3975

The influence of ground reflections on the measurement of aircraft engine exhaust noise is examined in this paper. A series of experiments were performed in the UCI aeroacoustic facility of supersonic jet noise with and without a ground plane in close proximity to the jet. Thus the effect of the ground plane on the radiated noise was isolated. Additionally, a computational model for the phenomenon was developed, which included the determination of a distribution of noise sources within the jet column. This distribution was developed from phased microphone array measurements incorporating an advanced beamforming algorithm. The developed model did a reasonably good job of predicting the effect of the reflecting ground surface. The most important exception is in the additional noise source caused by aerodynamic "scrubbing" of the turbulent jet on the surface far downstream of the jet exit. Guidance on how to alter the proposed model to account for porosity of the ground in field experiments over grassy or sandy terrain, is also given.

Nomenclature

a	=	Ambient speed of sound
A	=	Amplitude of Gaussian function
C_R	=	Complex reflectivity coefficient
D	=	Nozzle exit diameter
FNR	=	First frequency of negative reinforcement
f	=	Frequency in Hz
f_c	=	U/D, jet characteristic frequency
f_{NR}	=	Frequencies of negative reinforcement
h_j	=	Height of the jet axis from the ground
h_m	=	Height of the microphone from the ground
L	=	Length of the noise source region along jet axial coordinate
l	=	Distance of the direct path from the noise source to the microphone
M_d	=	Jet design Mach number
M_j	=	Jet Mach number
$OASPL$	=	Overall sound pressure level
P	=	Fourier transform of the pressure
p	=	Pressure measured by the microphone
Q	=	Fourier transform of the axial distribution of monopoles
q	=	Axial distribution of monopoles
R	=	Distance from the nozzle exit to the microphone
r	=	Distance of the reflected path

* Professor, Department of Aerospace Engineering, AIAA Fellow.
† Graduate Research Assistant, Department of Aerospace Engineering, AIAA Student Member.
‡ Professor, Department of Mechanical and Aerospace Engineering, AIAA Associate Fellow.

S_c = Power spectral density of the microphone signal in the absence of the ground
S_g = Power spectral density of the microphone signal in the presence of the ground
Sr = $f\,D\,/\,U$, Strouhal number
SPL = Sound pressure level
T_0 = Stagnation temperature
T_a = Ambient temperature
TR = $T_0\,/\,T_a$, Temperature ratio
t = Retarded time corresponding to the direct path
U = Jet exhaust velocity
X = Location of peak noise along jet axial coordinate
x = Position of the noise source along jet axial coordinate
β = Adjustable parameter
δ = Dirac delta function
θ = Polar angle measured from the jet axial coordinate
θ_i = Incidence angle (Fig.2)
ρ_1 = Density of air
ρ_2 = Density of the reflecting medium
τ = Time delay between the direct and reflected path arrival times
ω = Frequency in radians/s
Ψ = Autospectrum of the source distribution
ψ = Phase angle of reflectivity coefficient
ξ = Jet axial coordinate

I. Introduction

The radiated noise associated with high-speed jet engine exhausts continues to be a significant environmental and economic concern. High-speed jet noise remains a primary contributor of the overall aircraft noise for both commercial and military aircraft, especially at take-off. As efforts are made to change some aspect of the exhaust jets to obtain a noise benefit, the importance of being able to accurately measure the noise is crucial. This paper reports on a model study that tries to assess the influence of ground reflections on noise measured in field tests of actual aircraft undergoing noise exposure experiments. In these field tests the engine can be operated on an outdoor test stand, mounted on an aircraft that is fixed to a ground mounting system, or flying over an instrumented range. In such situations the microphones are often mounted some distance (like ~ 1 to 5 meters) above the ground (Gee [1] and Schlinker *et al.* [2]). The alternate widely used mounting system is one in which the microphones are located a small distance above a hard, flat plate. Acoustic pressure measurements are all multiplied by two for this arrangement as the reflection coefficient is unity, to engineering accuracy. (An example of this technique is well described in the paper by Seiner *et al.* [3].) The pole mounted microphones are used in efforts to minimize the influence of ground transmitted waves [4], refraction caused by near ground thermal gradients and/or uneven surfaces in the test area. In pole mounted microphones, however, noise that reaches the measuring microphones arrives from the indirect ground reflections as well as from the direct path. This paper addresses this ground reflection process.

Measured microphone spectra from field experiments show evidence of both positive and negative reinforcement as the path length differences match the specific (half) wavelengths. In addition, the integrated mean square value of the acoustic pressure is substantially increased in the vicinity of the exhaust jet noise sources. Although there are situations in which the noise of the aircraft produces an annoyance / hazard to the ground crews, the situation which affects the most people involves take-off or landing from airbases with nearby surrounding communities. Environmental impact studies of such airbases first require reasonably accurate estimates of the noise source characteristics (spectra and directivity) input into noise propagation models to properly predict the noise exposure on the ground.

Ground based measurements of the noise surrounding a turbojet engine will not accurately characterize the source description needed for a noise exposure prediction of an aircraft during landing or take-off unless the measurements are “corrected” for the ground reflections. Additionally the noise sources will be altered by forward flight effects, which is a topic not covered in this paper.

Attempts to estimate the contributions to measured noise signatures of the ground reflections have been developed and documented (ref. Pao *et al.*[4] and Salomons [5]). Such a decomposition, to be effective, needs to have reasonably accurate information of the spatial distribution of noise sources including the strong dependence on frequency that such sources have. Such data bases typically do not exist for the more recently developed aircraft engines (where they are needed most). One of the ways such data bases are established is with ground based aircraft engine experiments, which returns to the question of accurate accounting of the ground reflection influence.

The present study’s main goals were first, to provide experimental data and second, to develop a moderately simple model to derive “free field” noise source descriptions from measurements made in field experiments of turbojet engines. To meet the first goal a series of laboratory experiments of model scale exhaust jet flows was performed in the University of California Irvine aeroacoustics laboratory. A unique feature of these experiments was the performance of some of the measurements in the near vicinity of a flat plane located near to and parallel to the jet flow, to simulate a jet engine operating on a stand above the ground.

The second main goal was to develop a simple model to predict the effect of ground plane reflections on measured acoustic signals at positions located some distance above the ground. The development of such a model however, requires reasonably accurate information on the distribution of the noise sources within the jets. To provide this information an additional goal was added to perform measurements with an acoustic phased array to determine the distribution of noise sources within the jet. This technique employed an advanced beam forming algorithm developed by Papamoschou and Dadvar[6] .

In this study, the model jets all issue from a converging/diverging nozzle designed to provide relatively shock free flow at M_j =1.5. The jets were operated at the pressure ratio of 3.67 to produce this Mach number and two values of simulated temperature ratio, TR = 1.0 and 3.2. The jet condition was chosen to approximately match the conditions of the GE 414 engine which powers the F/A-18 aircraft (as reported by Seiner *et al.*[3]). It is this aircraft / engine combination that has recently been subjected to acoustic measurements both in fly-over and ground fixed set-ups; and more such experiments are anticipated.

Relating measurements of radiated noise from model jets in anechoic laboratories to those of full scale aircraft engines needs to follow quite precise methodology. To be rigorous in application, all parameters of the experiment or field test as well as the measured results are non-dimensionalized and properly matched between the conditions. In doing so, advantage is taken of the fact that the major features of the aeroacoustic phenomena are quite independent of Reynolds number, provided the Reynolds number of the experiment exceeds approximately 400,000 (Viswanathan[7]). In the non-dimensionalizing process it is important to make sure that frequency spectra of acoustic data, expressed as a function of Strouhal number = fD/U, satisfy Parseval’s condition that the integration of the spectra produce the appropriate measured overall sound pressure level (OASPL). It can also be appropriate to present laboratory measured spectra in terms of dimensional frequency scaled to the full size engine by simply reducing the frequency by the inverse scale ratio of the jet nozzle. In this paper we will show spectral data in both non-dimensional forms as well as in terms of frequency scaled to aircraft size.

A plot of acoustic spectra shown in Figure 1 clearly shows an extreme case of the problem with ground reflections in field experiments for aircraft size conditions. Shown in this figure are two spectra. One was reported by Gee *et al.*[8] in field tests of an F/A-18 aircraft in ground run-up with a single engine operating at mil spec conditions (without afterburner). The microphone was located 1.2 meters from the ground, 74 meters from the jet exhaust on a polar angle of 45 deg. from the downstream axis of the jet.

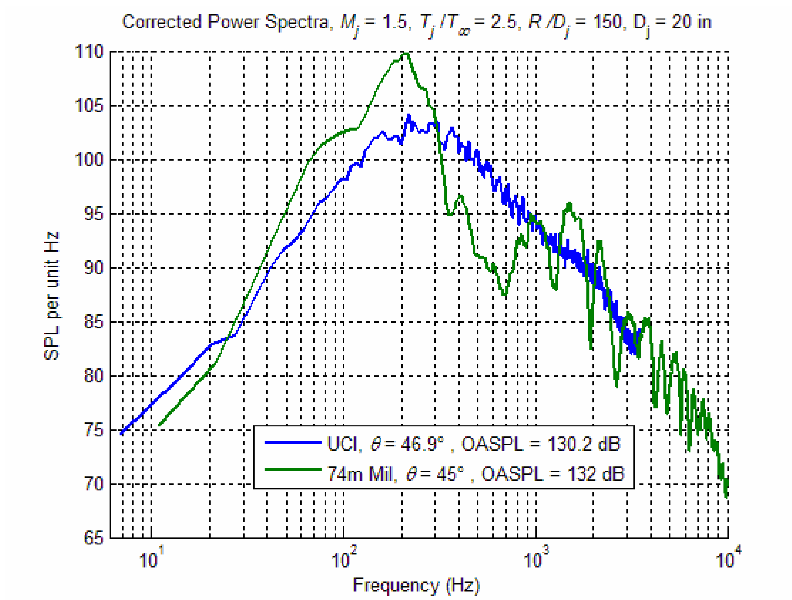

Fig.1 Comparison of acoustic measurements of aircraft jet engine noise with that of model jet in the laboratory anechoic chamber (scaled to aircraft frequency).

On the same (full scale) frequency plot is presented a microphone spectrum recorded in the UCI anechoic chamber with the jet nozzle operating at approximately the same Mach number and simulated temperature ratio. The frequency of these data has been scaled (down) by the appropriate scale ratio and the SPL per Hertz have been adjusted to preserve the integrated OASPL. Finally, the laboratory data, which were recorded at a microphone location of *R/D*=70 were scaled (by spherical spreading) to the *R/D* location of 150 corresponding to the aircraft measurements. This comparison shows that the difference in the spectral data conform to the character expected of the positive and negative reinforcement that has been described by Pao *et al.* [4], Salomons [5] and others. Additionally the integrated "overall" sound pressure level for the aircraft data demonstrate the net increase in acoustic energy as the positive re-enforcement exceeds the negative. Finally, the comparison shows remarkably good agreement in light of the facts that the size ratio is 35:1 and the aircraft data clearly show the effects of ground reflections. These ground influence features can be better understood following the summary of the analytical model described in the next section.

II. Model Development

In this section we develop a methodology for addressing the effect of a ground plane on the measurement of jet noise. We start from general relations and then apply them to a modeled jet noise distribution. The ground plane is treated as a flat solid surface – consistent with the setup of the experiment described in this paper. However, the methodology can easily be generalized for the case of soft or compliant ground by inserting the appropriate relationship for the reflectivity coefficient.

A. General Relations

The first step in the model development is to establish the geometric relationships for a point source, an observer microphone, and a ground plane. This analysis can be found in several prior works and is presented here for completeness. Figure 2 shows the geometric relationships and other relevant parameters.

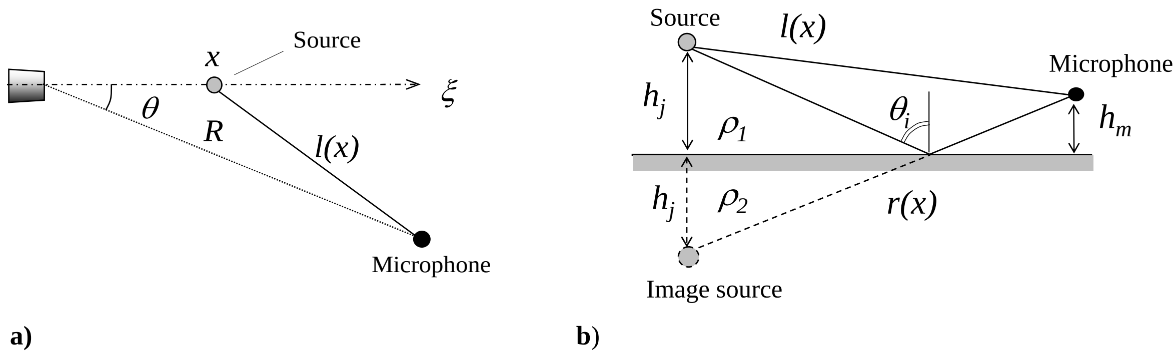

Fig. 2 Geometric relations of the jet, observer microphone and ground plane.
a) Top view; b) side view along *l*(x).

The coordinate system is centered at the nozzle exit. The microphone is at distance R from the nozzle exit and polar angle θ from the jet axis. The height of the jet axis from the ground is h_j and the height of the microphone from the ground is h_m. The reflected sound can be envisioned as coming from an image source at a height h_j below the ground. The density of the air is ρ_1 and the density of the reflecting medium is ρ_2. The incidence angle θ_i is used later in the reflectivity relations. The distance of the direct path from the noise source to the microphone is:

$$l(x) = \sqrt{(R\cos\theta - x)^2 + (R\sin\theta)^2} \tag{1}$$

and the distance of the reflected path can be shown to be

$$r(x) = \sqrt{l^2(x) + 4h_j h_m} \ . \tag{2}$$

The resulting time delay between the direct and reflected path arrival times is

$$\tau(x) = \frac{r(x) - l(x)}{a} \tag{3}$$

where a is the ambient speed of sound. Associated with this time delay are frequency values for positive and negative reinforcement, that is, frequencies for which the direct signal and the reflected signal originating from x are in phase or 180 deg out of phase, respectively. It is easy to show that the first frequency for negative reinforcement is

$$f_{NR}(x) = \frac{1}{2\tau(x)} = \frac{a}{2\left(r(x) - l(x)\right)} \quad . \tag{4}$$

Its nominal value, for x=0, is

$$f_{NR}(0) = \frac{a}{2\left(R - \sqrt{R^2 + 4h_j h_m}\right)} \tag{5}$$

and for $h_j h_m << R^2$,

$$f_{NR}(0) \approx a\frac{R}{4h_j h_m} \quad . \tag{6}$$

B. Line source

The next step is to establish the response of the microphone to an axially distributed source as depicted in Figure 3. In the following relations, t is the retarded time corresponding to the direct path. The jet noise source is modeled by an axial distribution of monopoles, $q(x,t)$.

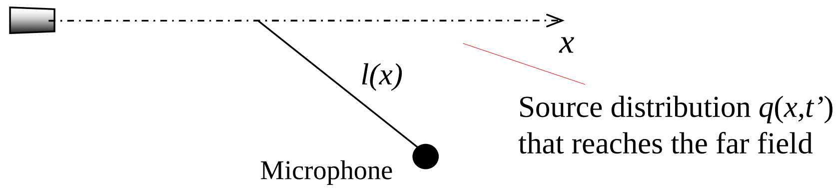

Fig.3 Schematic of coordinates for the sound source distribution.

The pressure measured by the microphone involves the axial integration of the direct and reflected (image) sound sources:

$$p(t) = \int_L \left(\frac{q(x,t)}{l(x)} + c_R \frac{q(x,t+\tau(x))}{r(x)} \right) dx \tag{7}$$

where L is the length of the noise source region and c_R is the complex reflectivity coefficient. Assuming $r(x) \approx l(x)$

$$p(t) = \int_L \frac{1}{l(x)} \left(q(x,t) + c_R q(x,t+\tau(x)) \right) dx \quad . \tag{8}$$

Taking the Fourier transform of the pressure

$$P(\omega) = \int_L \frac{1}{l(x)} Q(x,\omega) \left(1 + c_R e^{i\omega\tau(x)} \right) dx \ , \tag{9}$$

multiplying it by its complex conjugate and time averaging, we obtain the power spectral density of the microphone signal in the presence of the ground:

$$S_g(\omega) = \left\langle P(\omega) P^*(\omega) \right\rangle = \int_L \int_L \frac{1}{l(x) l(\xi)} \left\langle Q(x,\omega) Q^*(\xi,\omega) \right\rangle \left(1 + c_R e^{i\omega\tau(x)} \right) \left(1 + c_R^* e^{-i\omega\tau(x)} \right) dx d\xi \ . \tag{10}$$

The term $\left\langle Q(x,\omega) Q^*(\xi,\omega) \right\rangle$ is the cross-spectral density of the source. Assuming a spatially incoherent source distribution,

$$\left\langle Q(x,\omega) Q^*(\xi,\omega) \right\rangle = \Psi(x,\omega) \delta(x-\xi) \tag{11}$$

the spectrum simplifies to

$$S_g(\omega) = \int_L \frac{\Psi(x,\omega)}{l^2(x)} \left(1 + |c_R|^2 + c_R e^{i\omega\tau(x)} + c_R^* e^{-i\omega\tau(x)} \right) dx \ . \tag{12}$$

The function $\Psi(x,\omega)$ is the autospectrum of the source distribution and become the central parameter in the model that follows. Expressing the reflectivity coefficient in the form

$$c_R = |c_R| e^{i2\psi} \tag{13}$$

we obtain

$$S_g(\omega) = \int_L \frac{\Psi(x,\omega)}{l^2(x)} \left[1 + |c_R|^2 + 2|c_R| \cos\left(\omega\tau(x) + 2\psi \right) \right] dx \ . \tag{14}$$

The "clean" spectrum of the jet noise (no reflection) is

$$S_c(\omega) = \int_L \frac{\Psi(x,\omega)}{l^2(x)} dx \ . \tag{15}$$

Substituting in Eq. 14,

$$S_g(\omega) = \left(1 + |c_R|^2 \right) S_c(\omega) + 2|c_R| \int_L \frac{\Psi(x,\omega)}{l^2(x)} \cos\left(\omega\tau(x) + 2\psi \right) dx \tag{16}$$

and the ratio of the two spectra is

$$\frac{S_g(\omega)}{S_c(\omega)} = 1 + |c_R|^2 + \frac{2|c_R|}{S_c(\omega)} \int_L \frac{\Psi(x,\omega)}{l^2(x)} \cos\left(\omega\tau(x) + 2\psi\right) dx \ . \tag{17}$$

The maximum possible value of this ratio is

$$\left(\frac{S_g(\omega)}{S_c(\omega)}\right)_{\max} = 1 + |c_R|^2 + 2|c_R| \tag{18}$$

and the minimum possible value is

$$\left(\frac{S_g(\omega)}{S_c(\omega)}\right)_{\min} = 1 + |c_R|^2 - 2|c_R| \ . \tag{19}$$

C. Reflection from a Flat Solid Surface

For the case of reflection from a flat, non-porous solid surface, the reflectivity coefficient is given by [9]

$$c_R = \frac{1 + i(\rho_1/\rho_2)\tan\theta_i(x)}{1 - i(\rho_1/\rho_2)\tan\theta_i(x)} = e^{i2\psi(x)} \tag{20}$$

with

$$\psi(x) = \tan^{-1}\left[(\rho_1/\rho_2)\tan\theta_i(x)\right] \tag{21}$$

Here ρ is the density and θ_i is the incidence angle as defined in the Fig. 2. In other words, $|c_R|=1$ but there is a small phase shift due to the finite density ratio of the two media. The spectral ratio becomes

$$\frac{S_g(\omega)}{S_c(\omega)} = 2 + \frac{2}{S_c(\omega)} \int_L \frac{\Psi(x,\omega)}{l^2(x)} \cos\left(\omega\tau(x) + 2\psi(x)\right) dx \tag{22}$$

and its maximum and minimum possible values are 4 and 0, respectively. The geometric relation for the incidence angle is

$$\theta_i(x) = \frac{\pi}{2} - \frac{h_j + h_m}{l(x)} \ . \tag{23}$$

D. Model for Jet Noise

The nature and distribution of jet noise sources is a complex subject that is receiving intense investigation using experimental and analytical methods. Jet noise sources include sound generation due to turbulent mixing and shock-cell associated noise. Our jets contained both types of sources. Even though the jets were supposed to be perfectly expanded, imperfections in the nozzle design led to shock-cell noise, which was particularly noticeable in the broadside direction for pure air cold jets. The focus of this study is on turbulent mixing noise, which we model as a distribution of spatially-incoherent monopoles as per our analysis in Section C above. Such an approach risks oversimplification; nevertheless, it is the first "cut" in attempting to assess the impact of the ground plane on the measurement of jet noise.

The essence of our model is conveyed in the schematic diagram of Fig. 4. Based on current source localization measurements, and past measurements by other investigators, the peak value of the turbulent mixing noise source is far downstream of the jet exit for low frequency and moves towards the nozzle as the frequency increases. The locus of the peak noise is denoted $X(\omega)$. Centered around this locus is a distribution $\Psi(x,\omega)$ that decays with distance away from the locus. We approximate this distribution as a Gaussian. The width of the distribution is taken to be inversely proportional to the frequency.

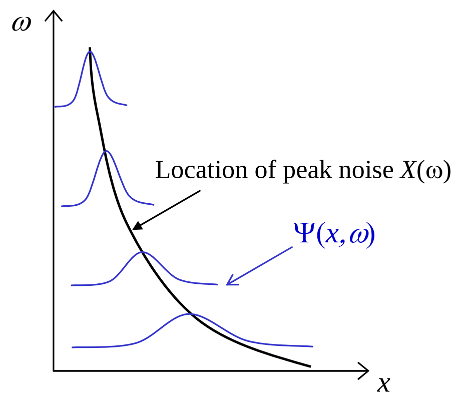

Fig. 4 Simple model for the distribution of turbulent mixing noise

The resulting expression for the source autospectrum is:

$$\Psi(x,\omega) = A(\omega)\exp\left(-\left[\beta\frac{\omega}{a}(x - X(\omega))\right]^2\right) \tag{24}$$

where β is an adjustable parameter. The distribution must satisfy Eq. 15 given earlier as:

$$S_c(\omega) = \int_{-\infty}^{\infty}\frac{\Psi(x,\omega)}{l^2(x)}dx \ . \tag{15}$$

Assuming $l \approx R$, integration of Eq. 15 yields

$$A(\omega) = \frac{R^2}{\sqrt{\pi}}\beta\frac{\omega}{a}S_c(\omega) \tag{25}$$

and we obtain

$$\Psi(x,\omega) = \frac{R^2}{\sqrt{\pi}}S_c(\omega)\beta\frac{\omega}{a}\exp\left(-\left[\beta\frac{\omega}{a}(x - X(\omega))\right]^2\right) \ . \tag{26}$$

Returning to the expression for the spectrum ratio (Eq. 22),

$$\frac{S_g(\omega)}{S_c(\omega)} = 2 + \frac{2\beta\omega}{a\sqrt{\pi}}\int_{-\infty}^{\infty}\exp\left(-\left[\beta\frac{\omega}{a}(x - X(\omega))\right]^2\right)\cos\big(\omega\tau(x) + 2\psi(x)\big)\,dx \,. \tag{27}$$

The spectral ratio of Eq. 27 will be compared with experimental values in the Section IV. The adjustable parameters are β and the locus of peak noise location $X(\omega)$.

III. Experimental Description

Experiments were conducted in the UCI Jet Aeroacoustics Facility [10]. The jet nozzle was designed by the method of characteristics for $M_d = 1.5$ flow and had an exit diameter of D = 14.2 mm. Air or helium-air mixtures were supplied to the nozzle at a total pressure of 360 kPa and exhausted inside an anechoic chamber (Fig. 5a). The ground plane was created by an acrylic plate of dimensions 1219×1219×12.7 mm. Its plane was parallel to the plane of the microphone array, described below. The plate was held at fixed position in the anechoic chamber, so the height of all the microphones was the same for all microphones and held constant at h_m = 50.8 mm (Fig. 5b). The jet height relative to the ground plane was variable and took the values h_j=50.8 mm and 69.9 mm. In terms of non-dimensional heights h/D, the microphone height (h_m / D = 3.6) and jet heights (h_j / D=3.6 and 4.9) are thought to be typical of those used in field testing of fighter aircraft.

Table 1 lists the tests configurations and flow conditions. Tests were performed on a "cold" Mach 1.5 jet, consisting of pure air, and a "hot" Mach 1.5 jet consisting of helium-air mixtures. The conditions of the "hot" jet represent are representative of the exhaust of a military afterburning turbofan engine.

Table 1. Exhaust conditions for M_j=1.5 jets

Designation	T_0/T_a	U (m/s)	Re_D
"Cold"	1.0	430	850,000
"Hot"	3.6	820	520,000

The microphone phased array consists of eight 3.2-mm condenser microphones (Bruel & Kjaer, Model 4138) arranged on a circular arc centered at the vicinity of the nozzle exit. The polar aperture of the array is 30 ^{o} and the array radius was 1 m. The microphones were all set at an angle to produce approximately normal incidence to the incoming acoustic waves. The angular spacing of the microphones is logarithmic. The entire array structure is rotated around its center to place the array at the desired polar angle. Positioning of the array is done remotely using a stepper motor. An electronic inclinometer displays the position of first microphone. By performing three experiments at identical conditions and rotating the entire 8 microphone array, a total aperture of 102 degrees (from 22 to 124 degrees) to the jet axis, was measured. The arrangement of the microphones inside the anechoic chamber, and the principal electronic components, are shown in Fig. 5a. The microphones were connected, in groups of four, to two amplifier/signal conditioners (Nexus 2690A OS4) with high-pass filter set at 300 Hz and low-pass filter set at 100 kHz. The four-channel output of each amplifier was sampled at 250 kHz per channel by a multi-function data acquisition board (National Instruments PCI-6070E). Two such boards, one for each amplifier, were installed in a Pentium 4 personal computer. National Instruments LabView software was used to acquire the signals. Even though the array provides noise source location maps, in this study it was used only to survey the far-field sound emitted by the jets. The sound pressure level spectrum was corrected for actuator response, free-field correction, and atmospheric absorption [11]. The overall sound pressure level (OASPL) was obtained by integrating the corrected spectrum. In some of the comparisons presented, the spectra were smoothed using a Savitzky-Golay filter [12].

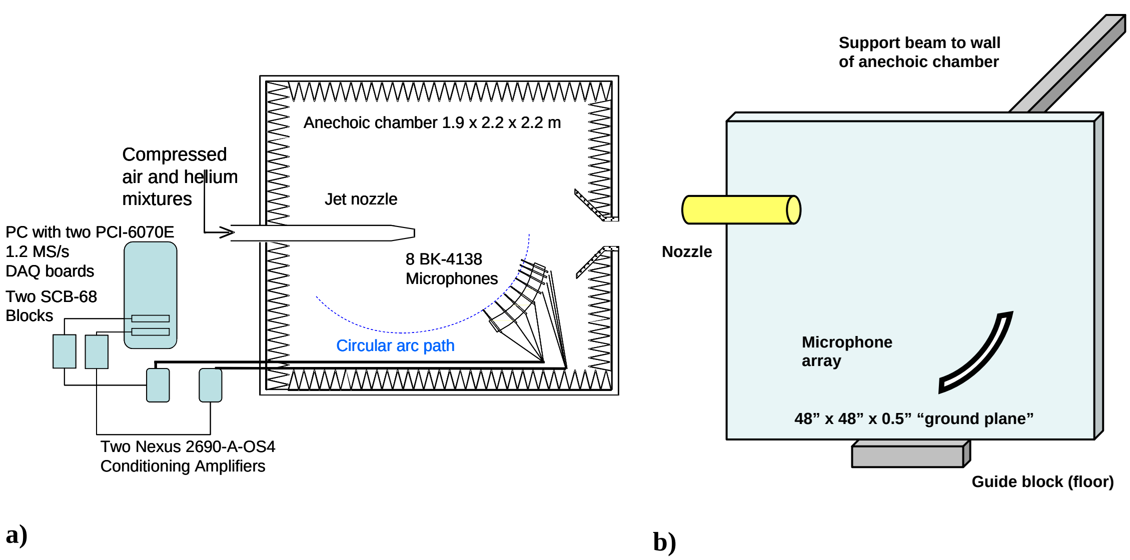

Fig. 5 a) Jet aerocoustics facility; b) simulation of ground plane.

IV. Results

The results are organized as follows. In Section A we present sound pressure level spectra with and without the ground plane to demonstrate the main effects of the ground plane. Next, in section B, we show acoustic source localization measurements that are used in the reflection model. Finally, Section C focuses on the ground-to-clean spectrum ratio S_g / S_c.

A. Effect of ground plane on sound pressure level spectra

The first data to show from the laboratory measurements are microphone spectra recorded at an angle of 32 degrees to the jet axis (Figure 6). Part a of the figure shows spectra recorded for the free jet and with the ground plane in place at a height of h_j/D= 3.6. In this case the jet is unheated (and has no helium in the jet gas mixture). The right panel of Fig. 6a shows comparative spectra for the simulated heated jet. Both of these comparisons clearly show the enhancement of the sound pressure levels at low frequencies below the value of frequency producing maximum negative reinforcement (FNR). The two observed prominent FNR values from these plots are 28 kHz and 30 kHz for the cold and simulated hot jets respectively. These convert to Sr = 1.1 and 0.7 for the cold and hot jets in non-dimensional frequency

"Cold" jet **"Hot" jet**

a) h_j/D=3.6

b) h_j/D=4.9

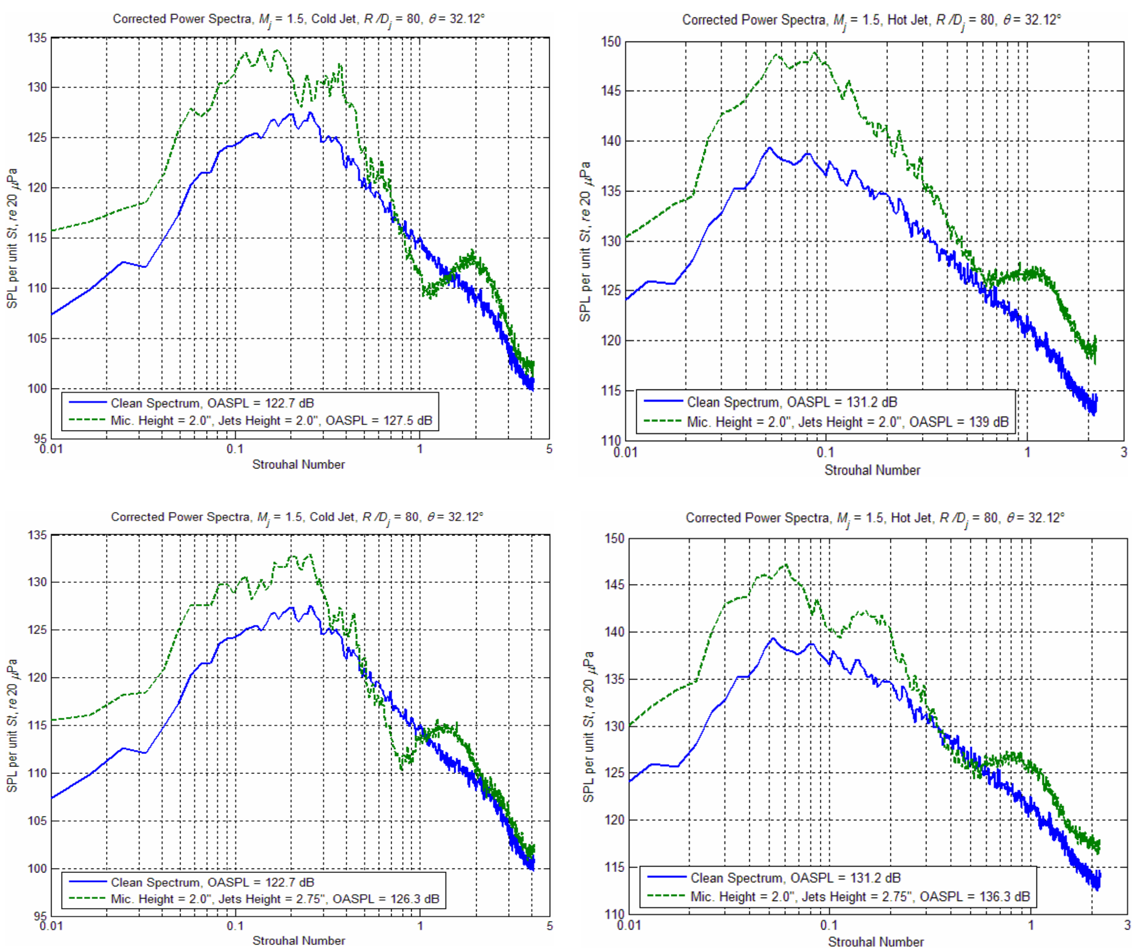

Fig. 6 Acoustic comparisons of clean jets and jets with ground plane at polar angle θ = 32 deg.

In general, the character of the spectra displayed in Figure 6 is quite like that observed by Gee *et al.* [1,8] in field experiments with both the F/A-18 and F-22 aircraft. A second series of our laboratory experiments on the jet noise in the proximity to a ground plane was conducted with the jet at a higher separation distance of $h_j / D = 4.9$ (Fig. 6 b). The microphones were maintained at the height of $h_m / D = 3.6$. The reduction of about 30 % in the FNR values compared with the data in Figure 6 a) is consistent with the increase in the jet height in turn by about 30 %.

B. Noise source localization measurements

The microphone array enabled noise source localization using delay-and-sum beamforming. The beamform map was deconvolved using the Richardson-Lucy inversion technique.[6] The deconvolved maps shown in Fig. 7 are based on the *complex coherence* of the acoustic field, rather than the cross-spectral density as is traditionally done. The details of this method will be presented in a future publication [13]. For the purposes of this paper, the coherence-based technique gives clearer maps of the evolution of the source distribution with frequency. These maps are shown for the cold and simulated hot jets. There is a clear trend of the noise source moving towards the nozzle exit as the frequency increases. For each Strouhal number, we can locate the axial position of the maximum value of the noise source distribution, $X(Sr)$. This is plotted in Fig. 8 for the hot and cold jet. There is only a small difference between the loci of the peak noise source for the two jets. (The peak noise of the hot jet occurs at $Sr = 0.2$ and that for the hot jet at $Sr = 0.15$.) The locus of the maximum noise source location can be approximated as

$$X(Sr) = \max(0\,, 5.1 - 7.3\log_{10} Sr) \tag{28}$$

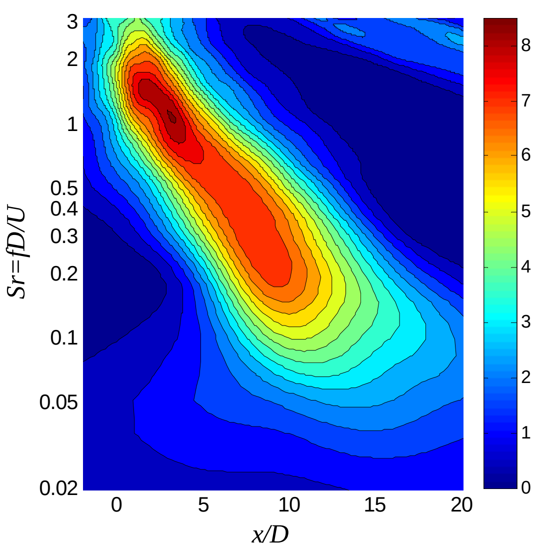

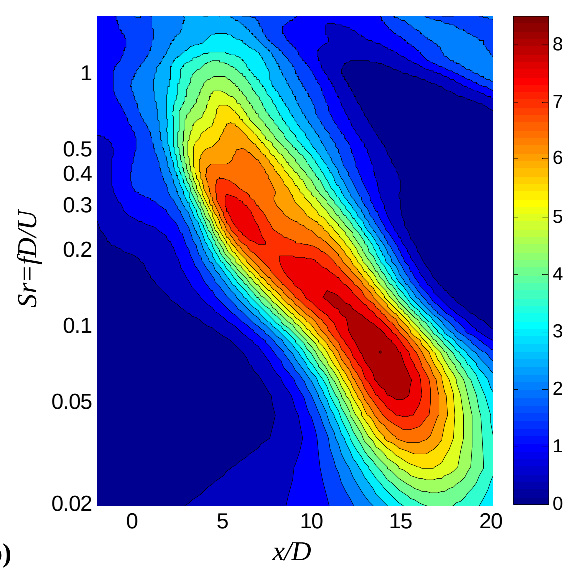

Fig. 7 Deconvolved, coherence-based noise source maps for the free jets for array aperture spanning from θ = 22 to 52 deg. a) Cold jet; b) Simulated hot jet.

This model is then used in the reflection model of Eq. 27. Around $X(Sr)$, the distribution decays similarly to the graphs of Fig. 4. In fact, Fig. 8 compares the actual distribution with the Gaussian model of Eq. 24 with $\beta = 0.5$. Reasonable agreement is found. The maps of Fig.7 also show global peaks of the noise source distribution. It is cautioned that these peaks *do not* represent the location of the global maximum of the noise source.

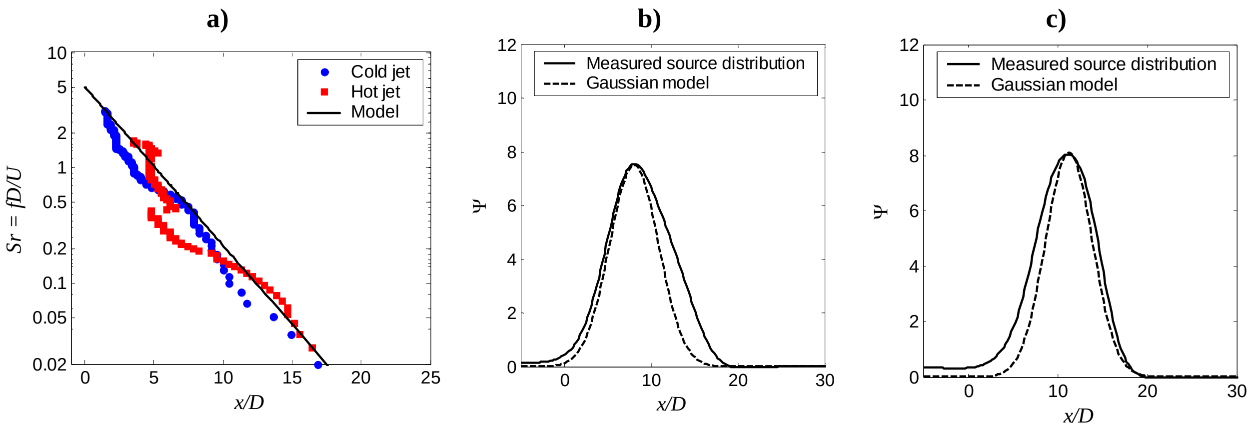

Fig. 8 Information extracted from the noise source maps of Fig. 7. a) Locus of peak noise with Strouhal number; b) distribution Ψ(*x*, *Sr* = 0.3) for cold jet; c) distribution Ψ(*x*, *Sr* = 0.15) for simulated hot jet.

C. Spectral ratio

We now have sufficient ingredients to test the model of Eq. 27 for the spectrum ratio S_g / S_c and compare with the experimental data. We will find upon doing so that all the processes involved result in a quite complicated situation. By designing an experiment with a controlled nearly perfect reflecting surface, we have simplified the process in a way that will prove to be an advantage when interpreting the experimental data. It is relatively easy to insert or remove the ground plane so that measurements made with it and without it can be conducted without changing any other parameter. (This is obviously not possible with a full size aircraft engine.) Initial examination of all spectral ratios shown in Figures 9 and 10 reveals that the analytical/empirical model presented in this paper does a reasonably good job of predicting the effect of the ground plane on the radiated noise for a portion of the spectra.

We find that the developed model does a very good job of predicting the spectral ratio (noise with ground plane over that without) in the frequency range of approximate maximum noise production and radiation. The model is too simple to predict the small wavelength noise, above a Strouhal number of about 1, which includes the higher harmonies of the first frequency of negative reinforcement (FNR). (This typically occurs at a noise level that is more than 20 dB below that at the maximum noise frequency.)

Close examination of the data of Figures 9 and 10 reveals that the present model substantially under-predicts the spectral levels below Strouhal number 0.3, particularly at low observation angles (measured from the jet axis). The discrepancy in noise levels (with the ground plane) are so substantial that it is clear that the present model is "missing" some important physics. We believe the missing physics is the aerodynamic interaction of the highly turbulent jet with the ground plane far downstream from the nozzle exit, but within the region of the acoustic far field measurements. This phenomenon has been referred to as "scrubbing noise" in prior works[14].

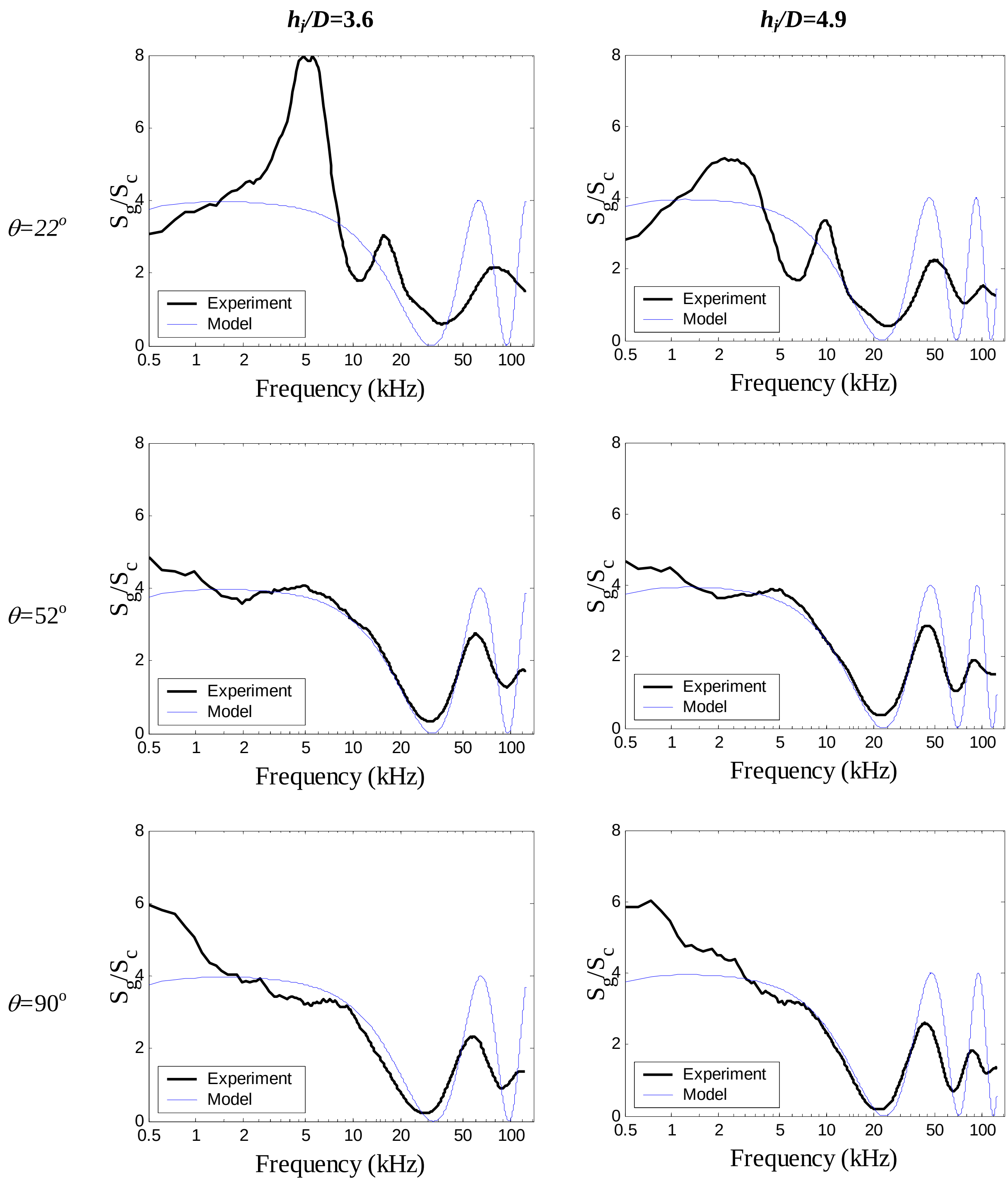

Fig. 9 Spectrum ratio S_g/S_c for the cold jet.

Jet scrubbing noise has been identified as a major noise source emanating from the trailing edge of a surface that shields jet noise[14]. One can imagine that this source is even stronger on the side of the surface that interacts directly with the jet. Isolated measurement of scrubbing noise would be very challenging because of the difficulty of separating it from the reflected jet noise (i.e., the same challenge as in the present work). Depending on the distance of the scrubbing area from the jet exit, the scrubbing noise may or may not be correlated with the jet noise source. Even a small correlation, however, would be enough to significantly upset the predictions of the peaks and valleys of the S_g/S_c model. It is possible that such interference creates the large departures between model and experiment seen at low polar angles in Figs. 9 and 10.

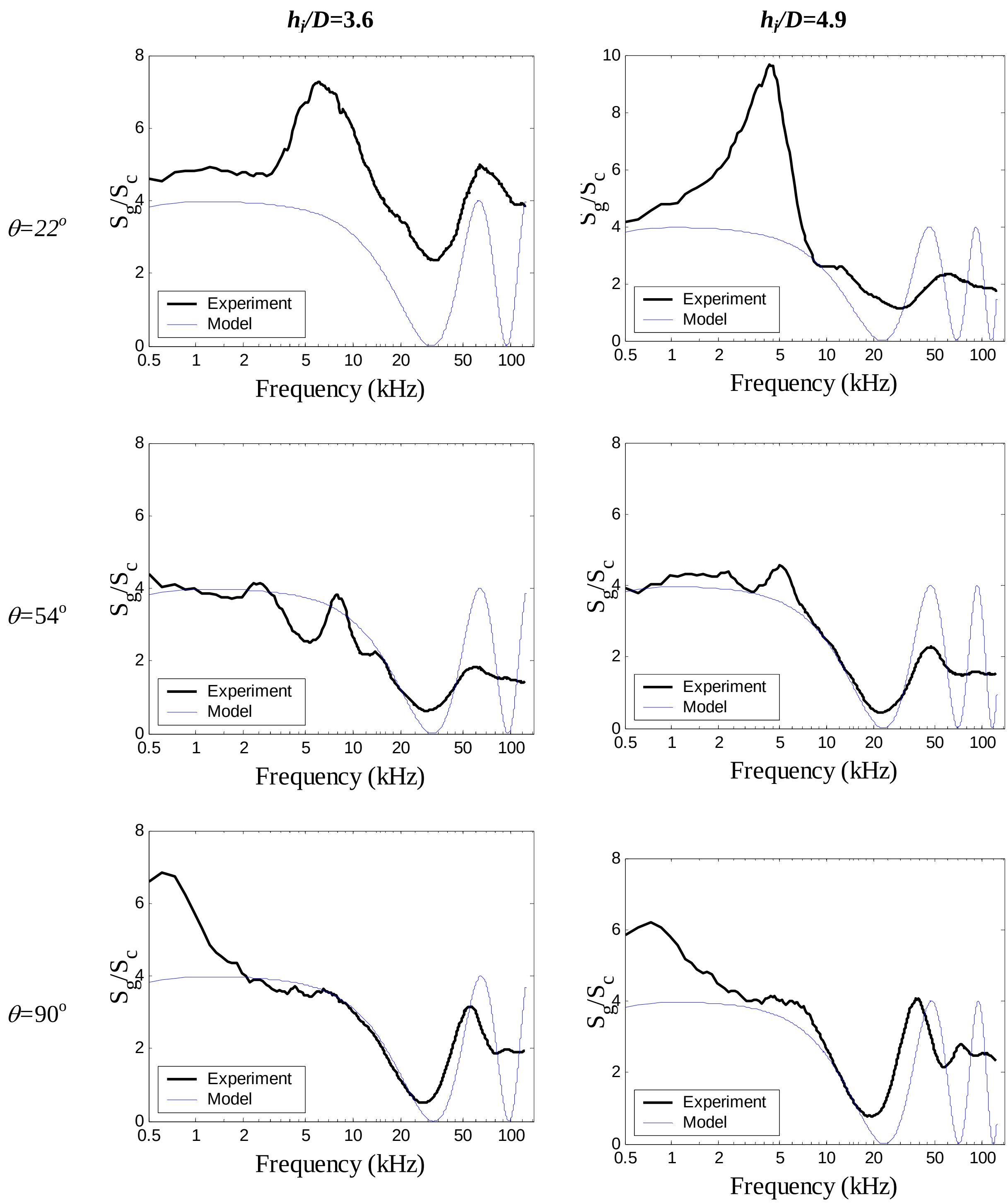

Fig. 10 Spectrum ratio S_g/S_c for the simulated hot jet.

We now turn our attention to potential application of the current model to the prediction of full size aircraft engine noise absent of the effect of ground reflections. There are two aspects of the measured noise that stand out. First is the anticipated excess noise (6 dB or more) at the low frequencies at which the reflection coefficient has values approaching 1. Second is the first (or fundamental) frequency of negative reinforcement (FNR). This is approximately calculated from Equation 6. In many cases simple efforts to correct the spectra at these locations should produce reasonable estimates of spectral shape at the location of maximum noise emission and the sideline (to the jet). The noise at angles closer to the jet axis will be poorly predicted because of the "scrubbing" noise.

We have the measured acoustic spectra and the approximate microphone and aircraft exhaust jet geometries as well as the operating conditions available from two sources reported in the literature. The microphone spectra reported for these cases show the characteristics discussed in this paper. The first of these is the result of experiments with an F-22 aircraft recorded at Edwards Air Force Base in a static propulsion test reported by Gee[1]. The relative geometries of the single operable engine, the proximity of the ground, the microphone location and the chosen polar angle are in close approximation proportionately to the presently reported laboratory experiments. The most prominent feature of the measured F-22 spectra is the quite noticeable dip in the spectral level at a frequency close to what is calculated by equation 6 for the FNR.

The spectrum shown in Figure 1 for the F/A-18 noise measurements reported by Gee *et al* [8] is examined for conformity to the currently proposed model. It is found that the calculated value of the FNR for the reported relative positions of the aircraft jet, the ground and the microphone for the conditions yielding the spectra shown in Figure 1, produce a predicted FNR of approximately 2,500 Hz. This is well above the spectral dips apparent in the frequency range from 300 to 1200 Hz. Discussion of these results with the authors of reference 8 revealed that attempts to correct for ground reflections would not be productive because of the uneven terrain of the test field, whose dimensions had not been mapped or documented. It appears that reflections from uneven terrain will have substantially greater influence on the spectral character of the radiated noise than can be predicted by the methods presented in this paper.

Finally some comments are in order relevant to the appropriate choice of complex reflection coefficient for experiments conducted over a grass field. Both Salomons[5] and Embleton *et al*.[15] report that the acoustic impedance of a grassy surface is best modeled by a flow resistivity model that incorporates the effect of surface porosity on both the real and imaginary components of the surface impedance. As a result of this, they show theoretical predictions of the negative reinforcement frequency (FNR) utilizing such a surface impedance model with optimized parameters. They show very good agreement between the theory and experiments as well. For geometric configurations not substantially different from the configurations we have been discussing in this paper, they showed that the FNR values are typically 20% lower than those obtained from calculations with a perfectly reflecting surface assumption. (These models however, cannot be used directly for aircraft noise propagation over a ground surface because they incorporate point acoustic sources rather than the extended aeroacoustic sources of a supersonic aircraft exhaust jet). The conclusion from this comparison demonstrates that Eq. 20 that we used in the present analysis for the reflection coefficient would need to be modified along the lines suggested by Salomons[5] and Embleton *et al*.[15] for accurate application to an aircraft experiment conducted over a surface not consisting of concrete.

V. Conclusions

By performing experiments in an anechoic chamber of the noise produced by a model supersonic exhaust jet with and without a ground plane, the effects of the reflections from the ground plane have been isolated. In developing a computational model of this phenomenon an important ingredient of this model has been shown to be a reasonably accurate distribution of noise source in the jet column. This was based on phased microphone array measurements incorporating an advanced beamforming algorithm.

From direct comparisons of far-field noise measurements made with and without the ground plane, it was established that the developed computational model did a reasonably good job of predicting the effect of the reflecting ground plate. The most important discrepancy, not predicted by the model, occurs in the low-to-mid frequency portion of the sound spectra at locations between 20 and 45 degrees from the jet axis. At such positions an additional noise source is evident in the measurements. It is thought that this source is caused by "scrubbing" of the turbulent jet on the surface far downstream of the jet exit plane. Guidance on how to alter the model to account for some porosity of the ground for field experiments over grassy or sandy terrain is also given.

VI. Acknowledgements

A portion of this work was performed under the sponsorship of the Strategic Environmental Research and Development Program. Dr. Micah Downing is acknowledged for suggesting this experiment some time ago, and Dr. Kent Gee provided data on the F/A-18 acoustic experiment.

References

[1] Gee, K.L., "Prediction of Nonlinear Jet Noise Propagation", PhD Thesis, Penn State University, University Park, PA, 2005.

[2] Schlinker, R.H., Liljenberg, S.A., Polak, D.R., Post, K.A., Chipman, C.T., and Stern, A.M., "Supersonic Jet Noise Characteristics and Propagation: Engine and Model Scale", AIAA Paper No. 2007-3623, 13th AIAA/CEAS Aeroacoustics Conference, Rome Italy. May, 2007.

[3] Seiner, J.M., Jansesn, B.J., Ukeiley, L.S., "Acoustic Fly-Over Studies of F/A E/F Aircraft During FCLP Mission," AIAA Paper 2003-3330, May 2003.

[4] Pao, S.P., Wenzel, A.R., and Oncley, P.B., "Prediction of Ground Effects on Aircraft Noise," NASA Technical Paper 1104, 1978.

[5] Salomons, E.K., "Computational Atmospheric Acoustics," Kluwer Academic Publishers, Dordrecht, 2001, pp.24, 118.

[6] Papamoschou, D., and Dadvar, A., "Localization of Multiple Types of Jet Noise Sources," AIAA Paper 2006-2644, May 2006.

[7] Viswanathan, K., "Does a Model Scale Nozzle Emit the Same Jet Noise as a Jet Engine?" AIAA Paper 2005-3936, May 2005.

[8] Gee, K.L., Sparrow, V.W., Gabrielson, T.B., Atchley, A.A., "Nonlinear Modeling of F/A-18E Noise Propagation", AIAA Paper No 2005-3089, 11th AIAA/CEAS Aeroacoustics Conference, Monterey, CA. May, 2005.

[9] Blackstock, D.T., "Fundamental of Physical Acoustics," Wiley, New York, 2000, p. 196

[10] Papamoschou, D. and Debiasi, M., "Directional Suppression of Noise from a High-Speed Jet", AIAA Journal, Vol. 39, No. 3, March 2001, pp. 380-387.

[11] Bass, H.E., Sutherland, L.C., Blackstock, D.T. and Hester, D.M., "Atmospheric Absorption of Sound: Further Developments", Journal of the Acoustical Society of America, Vol. 97, No. 1, 1995, pp. 680-683.

[12] Savitzky, A., and Golay, M.J.E., "Smoothing and Differentiation of Data by Simplified Least Squares Procedures," Analytical Chemistry Vol. 36, No.8, 1964, pp. 1627.

[13] Papamoschou, D., "Imaging of Directional Distributed Noise Sources," to be presented at the AIAA 14th Aeroacoustics Conference, May 2008.

[14] Von Glahn, U., Goodykoontz, J., and Wagner, J. "Nozzle geometry and forward velocity effects on noise for CTOL engine-over-the-wing concept," NASA TM-X-71453, Oct. 1973

[15] Embleton, T.F.W, Piercy, J.E., and Olson, N., "Outdoor Sound Propagation over Ground of Finite Impedance," Journal of the Acoustical Society of America, Vol. 59, No. 2, Feb. 1976.